Journal of *Marine Science and Engineering*

MDPI

Article

A New Calibration Method Based on Gravity-Assisted Navigation

Zhibo Zhou [1,2], Jianfeng Wu [1,3,4,*], Huabing Wu [1,3], Lintao Liu [2,*], Xinghui Liang [2], Hubiao Wang [2], Guocheng Wang [2], Junjian Lang [5], Zhimin Shi [2] and Xiaolong Guan [1]

1. National Time Service Center of the Chinese Academy of Sciences, Xi'an 710600, China; zhouzhibo@ntsc.ac.cn (Z.Z.); whb@ntsc.ac.cn (H.W.); guanxl@ntsc.ac.cn (X.G.)
2. State Key Laboratory of Precision Geodesy, Innovation Academy for Precision Measurement Science and Technology, Chinese Academy of Sciences, Wuhan 430077, China; lxh_whigg@asch.whigg.ac.cn (X.L.); wanghb@whigg.ac.cn (H.W.); guocheng96@apm.ac.cn (G.W.); shizhimin@whigg.ac.cn (Z.S.)
3. Key Laboratory of Time Reference and Applications, Chinese Academy of Sciences, Xi'an 710600, China
4. University of Chinese Academy of Sciences, Beijing 100049, China
5. The Department of Navigation Engineering, Naval University of Engineering, Wuhan 430033, China; langjunjian@apm.ac.cn

* Correspondence: wujianf@ntsc.ac.cn (J.W.); llt@asch.whigg.ac.cn (L.L.)

Abstract

Gravity-assisted navigation is an important means for underwater vehicles to achieve autonomous, passive, and long-endurance navigation. Among its key procedures, correcting the inertial navigation system (INS) based on gravity matching positions is of critical significance. In this paper, using shipborne measured INS data and gravity data together with a gravity database inverted from satellite altimetry data, the entire process of gravity-assisted navigation was experimentally validated through the normal time-frequency transform (NTFT) and Kalman filtering. NTFT is mainly used for gravity error correction, while Kalman filtering is primarily applied to matching algorithms. The analysis of the results shows that after 68.8 h, gravity-assisted navigation technology (GANT) can maintain navigation accuracy within 2 n mile (1 n mile ≈ 1852 m). Through comparison of different calibration methods, it is concluded that open-loop calibration applied only in the longitude direction is feasible and achieves satisfactory navigation performance. This surface vessel-based gravity-assisted navigation experiment addresses aspects such as experimental conditions and algorithmic techniques, serving as an important foundation for further underwater navigation applications.

Keywords: inertial navigation system; gravity-assisted navigation; gravity matching; normal time-frequency transform; Kalman filter; comprehensive correction

Check for updates

Academic Editor: Weicheng Cui

Received: 22 April 2026

Revised: 12 May 2026

Accepted: 15 May 2026

Published: 17 May 2026

1. Introduction

Navigation technology plays a vital role in both civilian and military fields. Different from the Global Navigation Satellite System (GNSS), the Inertial Navigation System (INS) offers distinct advantages, including autonomy, anti-interference capability, and the ability to provide high-frequency attitude, heading, velocity, and position information of the carrier [1], making it irreplaceable in certain applications, particularly in underwater navigation [2–4]. However, INS also has inherent limitations. As the errors of inertial sensors cannot be completely eliminated, the positioning error accumulates over time [5]. When performing long-endurance missions, once the error exceeds the acceptable range, the INS loses its effectiveness for navigation and positioning. Therefore, it is necessary to calibrate the INS using auxiliary information within permissible bounds. In terms of

 https://doi.org/10.3390/jmse14100925

auxiliary information sources, the gravity field is one of the fundamental physical fields of the Earth [6]. To a certain extent, it reflects information such as the Earth's internal structure and material migration. It is stable at the milligal scale and is geographically dependent, meaning that the gravity field contains geolocation information [7,8]. Consequently, if gravity matching technology is employed to obtain position information, the inertial navigation system can be calibrated. This is the basis of gravity-assisted navigation technology (GANT). Moreover, since the gravity field does not involve signal transmission issues, it is highly conducive to achieving autonomy and concealment for underwater vehicles [9].

The development of GANT is closely related to gravity measurement. In 1982, Bell Aerospace Textron successfully conducted gravity gradient measurement on a moving carrier using the Gravity Sensor System (GSS), and the GSS was installed on U.S. Navy equipment in the 1990s. Initially, it was used to measure the deflection of the gravity vector, and later it was applied to gravity-assisted navigation [9]. In reference [10], a traditional inertial navigation system was combined with a gravity gradiometer and a depth gauge to form a Gravity Aided Inertial Navigation System (GAINS), which can limit INS errors without the aid of external navigation devices. At the same time, the system can also be used to estimate the terrain around the carrier, enhancing safety while maintaining concealment, thereby improving long-endurance navigation capability. Lockheed Martin's Navigation and Gravity Systems (NGS) developed the low-cost Universal Gravity Module (UGM), which includes two types of gravity sensors: one gravimeter and three gravity gradiometers. The UGM is applicable to underwater weapons and also possesses terrain estimation capabilities. Reference [11] performed underwater dynamic gravity measurements using an INS, Doppler Velocity Log (DVL), and depth gauge (DG), achieving internal accuracies of 1.06 mGal and 0.89 mGal for two survey lines at a resolution of approximately 250 m.

The effectiveness of GANT is closely related to the gravity matching algorithm. Classical matching algorithms include Terrain Contour Matching (TERCOM), Iterated Closest Contour Point (ICCP), and Sandia Inertial Terrain Aided Navigation (SITAN) [12]. On this basis, many researchers have made improvements and innovations to these algorithms [13–15]. Meanwhile, the accuracy and resolution of the gravity database also have a significant impact on matching accuracy [16]. It is evident that a higher resolution and higher accuracy of the gravity database lead to improved final matching accuracy. Reference [17] researched the effect of gravity database on navigation accuracy, computationally analyzed the simulated and measured data by using the Kriging interpolation method, and investigated the effect of gravity database density on navigation results.

After obtaining the gravity matching position, comprehensive calibration is a key step in suppressing INS errors. The problem of compensation of vertical deviation and the gravity navigation technique was discussed in [18]; the latter sensor includes gravimeter and gravity gradiometer, and pointed out that open-loop and closed-loop calibration can be applied, in which the open-loop calibration acts directly on the output result, and the simplicity of the construction is the advantage, but the closed-loop calibration can also realize the estimation of inertial device error, and the algorithms used are Extended Kalman Filter (EKF), which allows for passive navigation. For cases where the matching positions are continuous and sparse, the EKF and multi-point calibration algorithm were respectively designed in [19], which are also two representative algorithms.

In the aforementioned studies, closed-loop calibration using Kalman filtering is commonly adopted when matched positions are available. However, in practical gravity-assisted navigation scenarios, the matched positions are inherently sparse and irregular, and their accuracy may be degraded in regions where the gravity field lacks distinctive spatial features. Under such conditions, a Kalman filter operating in the correction loop faces the risk of divergence during long measurement gaps. Moreover, the INS velocity contains inherent Schuler and Foucault periodic oscillations, which can propagate through the matching loop and degrade the calibration performance. To tackle these problems, this paper proposes a new calibration method with two main contributions.

The main contributions of this work are twofold. First, the NTFT is applied in a gravity-assisted navigation system. By extracting and removing the Schuler periodic oscillation from the INS velocity before it enters the matching loop, the Foucault oscillation is simultaneously suppressed due to the modulation relationship between the two, thereby reducing the oscillatory errors that would otherwise propagate into the matched position. Second, a direct position reset correction strategy is proposed, in which the matched position directly overwrites the INS position. This open-loop correction approach avoids the divergence risk associated with Kalman filtering fusion under the sparse and low-accuracy measurement conditions typical of gravity-assisted navigation.

The paper is organized as follows: Section 1 introduces the background; Section 2 describes the methodology and data processing workflow, specifically including system composition, INS mechanization and error characteristics, gravity measurement, gravity database, gravity matching, and INS calibration. Section 3 is the shipborne experiment. Section 4 is the discussion. Section 5 is the conclusion.

2. Methodology and Data Processing Workflow

2.1. System Composition

This paper validates the gravity-assisted navigation technology (GANT) using shipborne measured data, with an emphasis on comparing the impact of different calibration methods on the final navigation results. The gravity-assisted navigation system mainly consists of navigation equipment, a gravity measurement system (GMS), a gravity database, and matching algorithms. The data processing flow is shown in Figure 1. Common underwater navigation equipment includes the INS, Doppler velocity log (DVL), and depth gauge (DG). Among these, the DVL can provide velocity-aiding information, and the DG can provide depth information. Since they were not used in this experiment, they are not listed in Figure 1.

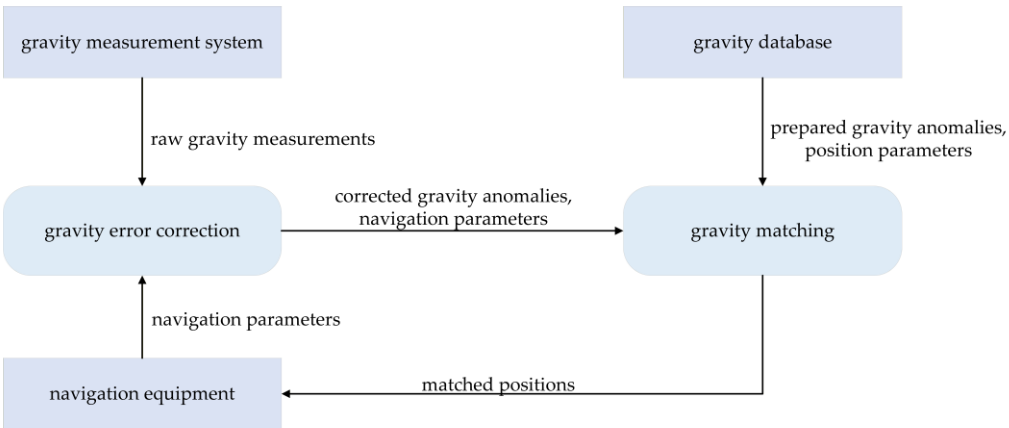

Figure 1. Data processing flow chart of gravity-assisted navigation system.

The GMS provides raw gravity measurements, while the navigation equipment supplies navigation parameters for gravity error correction. Subsequently, the gravity matching algorithm matches the corrected gravity anomalies with the gravity database to obtain the matched position. The gravity database is the Sandwell et al. [20] global marine gravity model, which is derived from multi-satellite radar altimetry data and has a grid spacing of 1 arcminute with an accuracy of approximately 2 mGal over most ocean areas. These matched positions are then fed back to the INS for calibration, thereby enabling autonomous passive long-term navigation. Various calibration strategies exist for INS calibration; this paper adopts open-loop calibration, which calibrates only the INS outputs.

2.2. INS Mechanization and Error Characteristics

INS is based on Newton's laws of motion, with gyroscopes and accelerometers as its two core components: the former provides angular motion information, while the latter provides linear motion information. Describing the state of motion in space requires a frame of reference, which is typically represented by a coordinate system. Moreover, since the same vector has different representations in different coordinate systems, it is necessary to introduce spatial transformation relationships between coordinate systems.

The Earth-centered inertial frame (denoted as the i-frame) has its origin at the Earth's center. Its x-axis points toward the vernal equinox, its z-axis aligns with the Earth's rotation axis, and its y-axis completes a right-handed Cartesian coordinate system together with the x- and z-axes. The measurements from gyroscopes and accelerometers are expressed relative to the i-frame.

The Earth-centered Earth-fixed frame (denoted as the e-frame) has its origin at the Earth's center. Its x-axis points toward the prime meridian, its z-axis aligns with the Earth's rotation axis, and its y-axis completes a right-handed Cartesian coordinate system together with the x- and z-axes.

The navigation frame (denoted as the n-frame) has its origin at the center of the carrier. Its x-axis points to geographical east, its y-axis points to geographical north, and its z-axis completes a right-handed Cartesian coordinate system together with the x- and y-axes, forming the common east-north-up (ENU) coordinate system.

The body frame (denoted as the b-frame) has its origin at the center of the carrier, with its x-axis pointing to the right, its y-axis pointing to the front, and its z-axis completing a right-handed Cartesian coordinate system together with the x- and y-axes.

Transformations between different coordinate frames can be represented using a direction cosine matrix (DCM). For example, the matrix C_i^n represents the relationship between the i-frame and the n-frame. The coordinate system provides the reference for INS mechanization. Next, the INS update solution equations are given, expressed in the n-frame.

The attitude update equation is introduced as shown in Equation (1).

$$\dot{C}_b^n = C_b^n \left(\omega_{nb}^b \times \right) \tag{1}$$

where C_b^n represents the relationship between the b-frame and the n-frame, $\dot{C}_b^n$ represents the differential of C_b^n, ω_{nb}^b represents the projection of the angular velocity of the b-frame relative to the n-frame onto the b-frame, $\omega_{nb}^b \times$ denotes the skew-symmetric matrix of ω_{nb}^b.

From the vector composition principle of angular velocity, the following kinematic relation is obtained:

$$\omega_{nb}^b = \omega_{ib}^b - \omega_{in}^b \tag{2}$$

thus, Equation (1) can be further expressed as follows:

$$\dot{C}_b^n = C_b^n \left(\omega_{ib}^b \times \right) - (\omega_{in}^n \times) C_b^n \tag{3}$$

where ω_{ib}^{b} is the measured value of the gyroscope, ω_{in}^{n} represents the projection of the angular velocity of the n-frame relative to the i-frame onto the n-frame, which can be further expressed as shown in Equation (4).

$$\omega_{in}^{n} = \omega_{ie}^{n} + \omega_{en}^{n} \tag{4}$$

where ω_{ie}^{n} denotes the projection of the angular velocity of the Earth's rotation into the n-frame, and ω_{en}^{n} denotes the projection of the angular velocity of the rotation of the n-frame with respect to the e-frame into the n-frame. Their specific expressions are shown in Equations (5) and (6).

$$\omega_{ie}^{n} = \begin{bmatrix} 0 & \omega_{ie}\cos L & \omega_{ie}\sin L \end{bmatrix}^{T} \tag{5}$$

$$\omega_{en}^{n} = \begin{bmatrix} \frac{-v_N^n}{R_M+h} & \frac{v_E^n}{R_N+h} & \frac{v_E^n \tan L}{R_N+h} \end{bmatrix}^{T} \tag{6}$$

where ω_{ie} denotes the magnitude of the Earth's rotation angular velocity, $\omega_{ie} = 7.2921151467 \times 10^{-5}$ rad/s; L represents the latitude; v_E^n and v_N^n represent the east and north velocities, respectively; R_M represents the meridian radius of curvature of the ellipsoid; R_N represents the normal radius of curvature of the ellipsoid; and h represents the height.

The velocity update equation is shown in Equation (7).

$$\dot{v}_{en}^{n} = C_b^n f^b - (2\omega_{ie}^{n} + \omega_{en}^{n}) \times v_{en}^{n} + g^n \tag{7}$$

where f^b denotes the accelerometer measurement, $\dot{v}_{en}^{n}$ represents the differential of v_{en}^{n}, and g^n represents the gravity vector in the n-frame.

Integrating velocity yields position, and the position update equation is expressed as follows:

$$\begin{cases} \dot{L} = \frac{v_N}{R_M+h} \\ \dot{\lambda} = \frac{v_E}{R_N+h}\sec L \\ \dot{h} = v_U \end{cases} \tag{8}$$

where λ represents the longitude, v_U represents the up velocity.

The INS error equations are commonly used to analyze error characteristics. The altitude channel of the INS is divergent and typically requires external measurement information from other devices; alternatively, if the altitude does not vary significantly, it can be set to a constant value. Excluding the velocity and position errors in the up direction, the remaining errors—namely, the attitude angle errors, the east and north velocity errors, and the latitude and longitude errors—are expressed as follows.

$$\dot{\phi}_E = \left(\omega_{ie}\sin L + \frac{v_E \tan L}{R_{Nh}}\right)\phi_N - \left(\omega_{ie}\cos L + \frac{v_E}{R_{Nh}}\right)\phi_U - \frac{\delta v_N}{R_{Mh}} - \varepsilon_E \tag{9}$$

$$\dot{\phi}_N = -\left(\omega_{ie}\sin L + \frac{v_E \tan L}{R_{Nh}}\right)\phi_E - \frac{v_N}{R_{Mh}}\phi_U + \frac{\delta v_E}{R_{Nh}} - \omega_{ie}\sin L\delta L - \varepsilon_N \tag{10}$$

$$\dot{\phi}_U = \left(\omega_{ie}\cos L + \frac{v_E}{R_{Nh}}\right)\phi_E + \frac{v_N}{R_{Mh}}\phi_N + \frac{\tan L\delta v_E}{R_{Nh}} + \left(\omega_{ie}\cos L + \frac{v_E \sec^2 L}{R_{Nh}}\right)\delta L - \varepsilon_U \tag{11}$$

$$\begin{aligned} \delta\dot{v}_E = &-f_U\phi_N + f_N\phi_U + \tfrac{v_N \tan L}{R_{Nh}}\delta v_E + \left(2\omega_{ie}\sin L + \tfrac{v_E \tan L}{R_{Nh}}\right)\delta v_N + \\ &\left(2v_N\omega_{ie}\cos L + \tfrac{v_E v_N \sec^2 L}{R_{Nh}}\right)\delta L + \nabla_E \end{aligned} \tag{12}$$

$$\dot{\delta v_N} = f_U\phi_E - f_E\phi_U - 2\left(\omega_{ie}\sin L + \frac{v_E \tan L}{R_{Nh}}\right)\delta v_E - v_E\left(2\omega_{ie}\cos L + \frac{v_E \sec^2 L}{R_{Nh}}\right)\delta L + \nabla_N \tag{13}$$

$$\dot{\delta L} = \frac{\delta v_N}{R_{Mh}} \tag{14}$$

$$\dot{\delta\lambda} = \frac{\delta v_E \sec L}{R_{Nh}} - \frac{v_E \sec L \tan L}{R_{Nh}}\delta L \tag{15}$$

where $\phi = \begin{bmatrix}\phi_E & \phi_N & \phi_U\end{bmatrix}^T$ represents the attitude angle error, and $\dot{\phi}$ represents the differential of ϕ; δv_E and δv_N represent the east velocity error and north velocity error, respectively, and $\dot{\delta v_E}$ and $\dot{\delta v_N}$ represent the differentials of δv_E and δv_N; δL and $\delta\lambda$ represent the latitude error and longitude error, respectively, and $\dot{\delta L}$ and $\dot{\delta\lambda}$ represent the differentials of δL and $\delta\lambda$; $f = \begin{bmatrix}f_E & f_N & f_U\end{bmatrix}^T$ represents specific force.

Combining the INS updating equations and error equations reveals that the attitude, velocity, and position navigation parameters are coupled and mutually influential; however, the longitude error is relatively independent and does not couple into the other navigation error parameters as a separate error source. This provides an approach for the selection of calibration schemes.

2.3. Gravity Measurement

Gravity measurements are carried out aboard the ship using a gravimeter. Gravity is one of the fundamental data sources for gravity-assisted navigation and is also an important factor affecting the accuracy of gravity matching. As illustrated in Figure 2, converting raw gravity measurements into gravity products—typically gravity anomalies—requires signal conversion and error correction [21].

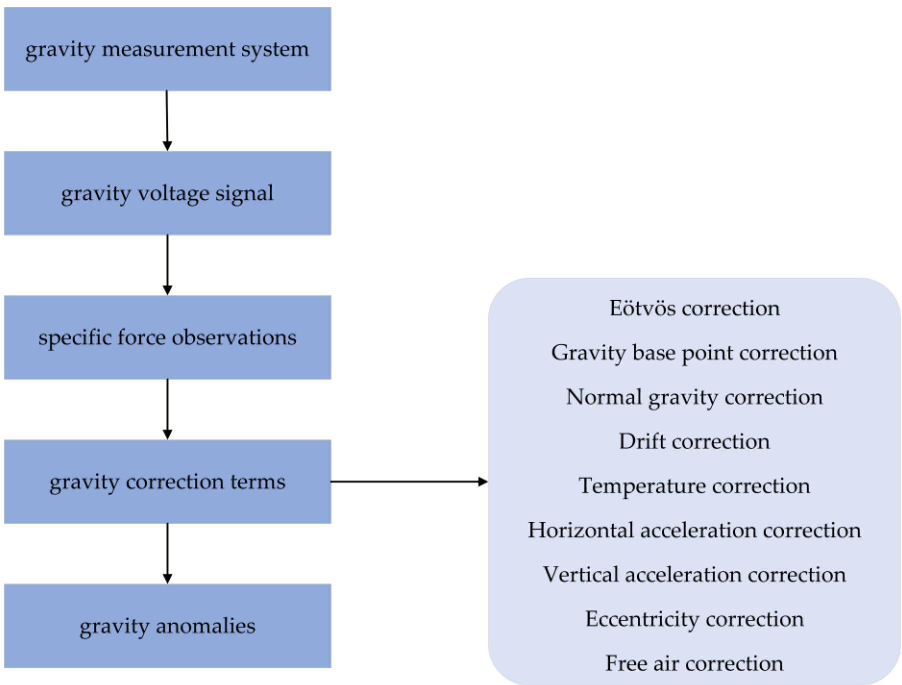

Figure 2. Gravity data processing flow and error correction.

Error correction is critical, and the most influential corrections are drift correction, normal gravity correction, and the *Eötvös* correction. Among these, the *Eötvös* correction is the key factor affecting the accuracy of gravity anomalies. The correction formula is shown in Equation (16).

$$\delta g_e = 2v_E \omega_{ie} \cos L + \frac{{v_E}^2}{R_{Nh}} + \frac{{v_N}^2}{R_{Mh}} \tag{16}$$

where $R_{Nh} = R_N + h$, $R_{Mh} = R_M + h$. Equation (16) shows that the *Eötvös* correction depends on both velocity and latitude. In fact, the INS latitude error oscillates around a certain constant value. Although the oscillation amplitude gradually increases due to inertial sensor errors, its influence on the Eötvös correction is limited. Velocity remains the most influential factor.

In data processing, to better simulate the underwater environment, auxiliary information from other devices is avoided as much as possible; only the navigation parameters provided by the INS are used for gravity error correction. Due to the Schuler period oscillation in the velocity and latitude obtained from pure INS, this paper first employs the NTFT to suppress the Schuler period oscillation error [22], and then applies it to gravity error correction.

Figures 3 and 4 show a comparison of east and north velocities between pure INS and those NTFT-processed, and "NTFT-processed" means after being processed by NTFT. The comparison clearly demonstrates that NTFT suppresses the Schuler period oscillation error in pure INS.

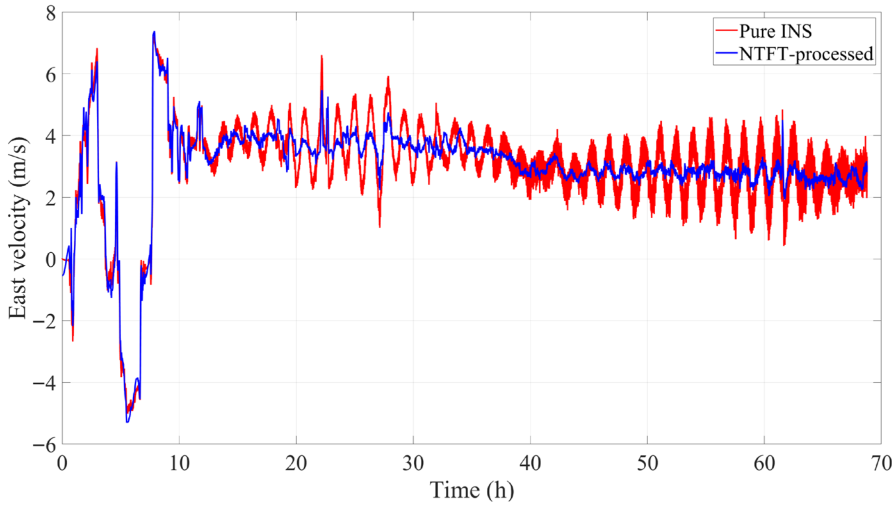

Figure 3. Comparison of east velocities for different calculation methods.

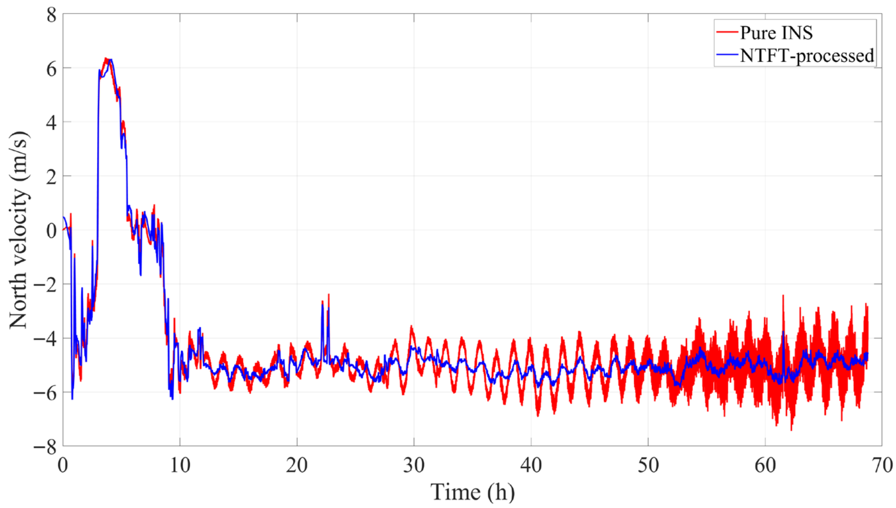

Figure 4. Comparison of north velocities for different calculation methods.

If the pure INS parameters, including velocity and latitude, are used directly for gravity error correction, the Schuler period oscillation will inevitably be introduced into the gravity signal, resulting in gravity measurement errors. If the test area itself has little gravity variation, the true gravity signal will be overwhelmed by these errors. As shown in Figure 5, the gravity change is more pronounced between approximately the 35th and 47th hours, which corresponds to passing through a trench, and it also shows that there is a strong correlation between gravity and topography.

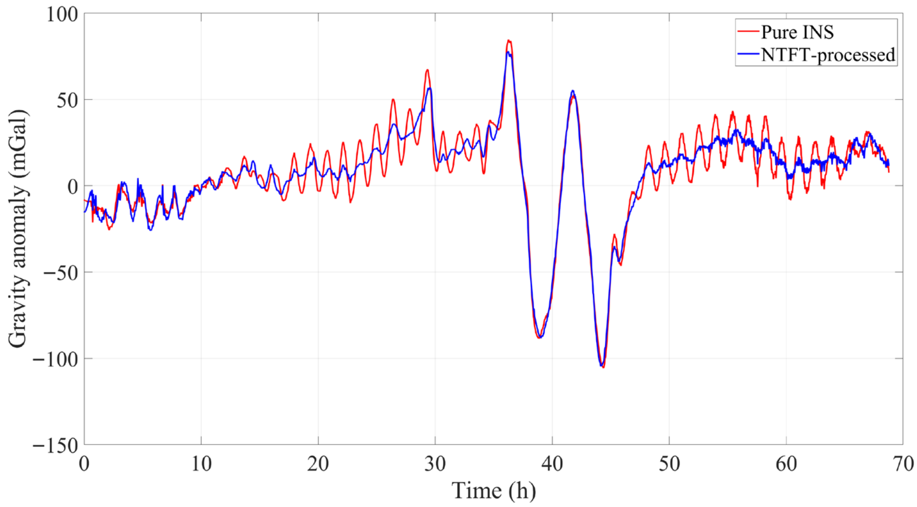

Figure 5. Comparison of gravity anomaly for different calculation methods.

2.4. Gravity Database

The gravity database is an important data source in gravity-assisted navigation, and its resolution and accuracy directly affect the gravity matching performance. Gravity database can be acquired through various measurement methods, including satellite, airborne, and shipborne gravimetry. Among these, satellite gravimetry enables large-scale coverage but offers limited resolution and accuracy. Airborne and shipborne gravimetry can provide richer gravity information; however, they are expensive and time-consuming. Consequently, the final gravity database is typically constructed by fusing multi-source data with the aid of interpolation methods.

Due to the current unavailability of airborne and shipborne gravity data for the corresponding regions, this paper uses only gravity anomalies derived from satellite altimetry data inversion. The data were released by the David T. Sandwell team at the Scripps Institution of Oceanography [20,23], with a resolution of $1' \times 1'$ and are available at https://topex.ucsd.edu/grav_outreach/ (accessed on 10 November 2023), where a more detailed description can be found. Only a portion of the area is selected here, as shown in Figure 6. In the figure, the background image represents the gravity anomaly, the red line indicates the actual trajectory of the ship, and the black arrow indicates the direction of travel. This region includes both areas with relatively smooth gravity variations and areas with relatively drastic changes, making it somewhat representative. The black box in Figure 6 marks the trench-crossing area, where the gravity change is very pronounced, with an amplitude exceeding 150 mGal. This is consistent with the results shown in Figure 5.

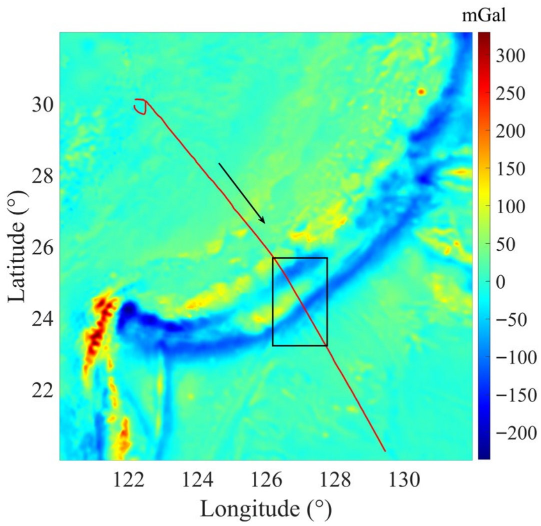

Figure 6. Shipborne test track and gravity anomaly over the traversed area.

2.5. Gravity Matching

The gravity matching algorithm is a key technology for enabling gravity-assisted navigation. Its function is to match the measured gravity data with the stored gravity database to obtain a position estimate with higher accuracy. In this paper, gravity matching is performed using an optimized SITAN method, where the INS-indicated position serves as the search center, and the search is conducted within a radius corresponding to a certain confidence level. The matching position is then calculated via parallel Kalman filtering. This matching method is insensitive to velocity and heading errors, as shown in [24].

2.6. INS Calibration

GANT is a comprehensive calibration method aimed at improving the long-term navigation capability of INS. It represents a form of generalized integrated navigation, differing from INS/GNSS integrated navigation in that the position information provided by gravity-assisted navigation has uneven and relatively long time intervals and lower accuracy. In this paper, the inertial sensor errors are not estimated; instead, only an open-loop calibration of the INS position error is performed, which is equivalent to a position reset.

3. Shipboard Test

The shipboard test was carried out aboard the Da Yang Hao research and survey vessel. A self-developed gravimeter, designated the CHZ-II ocean gravimeter, was installed in the gravity chamber and received GNSS signals via a serial port. A strapdown INS was installed adjacent to the gravimeter, with a gyroscope bias accuracy better than 0.003 °/h and an accelerometer bias accuracy better than 20 μg. The installation configuration of the CHZ-II and the INS is shown in Figure 7.

As shown in Figures 8 and 9, the matching error is compared with the pure INS error, with the horizontal coordinate representing the matching sequence number. From the matching results, it can be seen that at the initial stage, the matching error is relatively large with obvious jumps. This is partly because, in coastal areas, the gravity database accuracy is degraded by the proximity to offshore regions, as well as by land contamination and tidal model errors affecting satellite altimetry data [25], and partly because the Kalman filter algorithm requires a certain amount of convergence time.

Figure 7. Shipborne gravity-assisted navigation system.

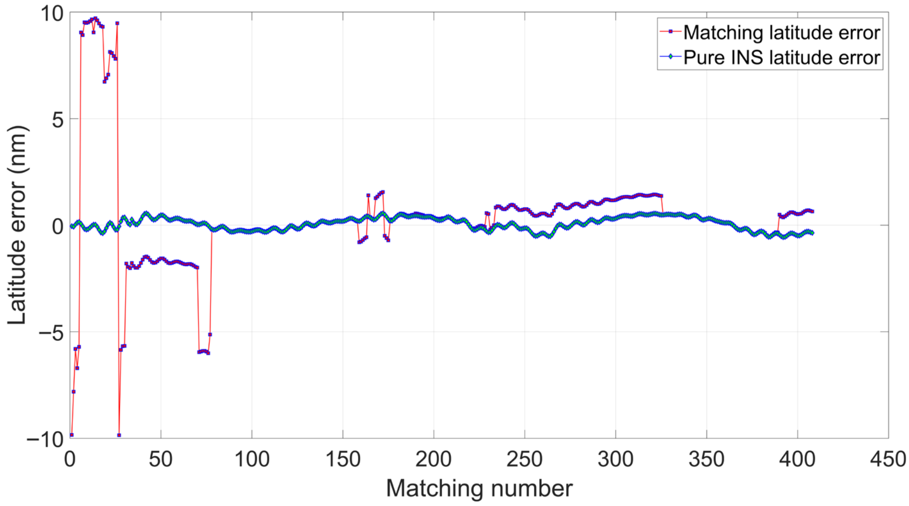

Figure 8. Pure INS error and matching error in the latitude direction.

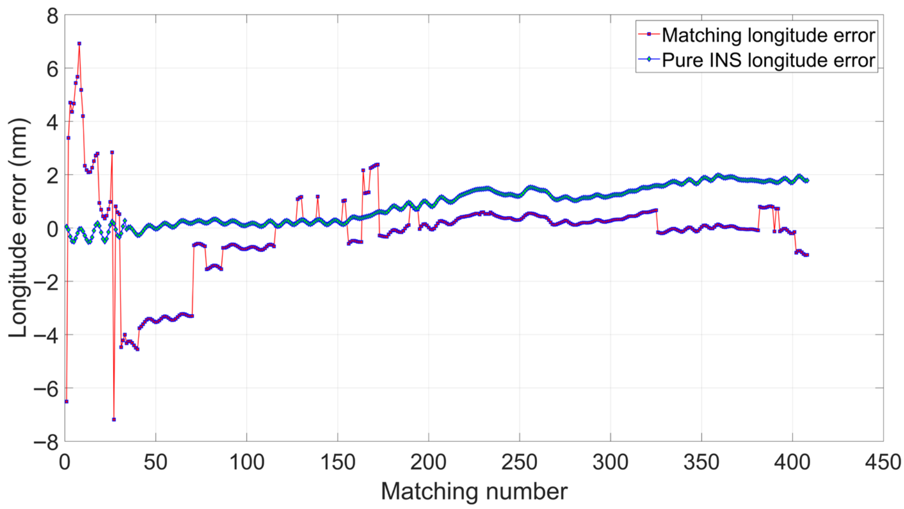

Figure 9. Pure INS error and matching error in the longitude direction.

For latitude error, the accuracy is not significantly improved; in some areas, the matching accuracy is even lower than that of pure INS. For longitude error, both positive and negative errors occur, and the matching accuracy varies—sometimes high, sometimes low. Overall, however, the accuracy is clearly improved. In practice, higher matching accuracy is certainly desirable, as it directly affects the effectiveness of INS comprehensive calibration and influences the selection of calibration strategies. Ultimately, maximizing the gravity-assisted navigation accuracy based on a given matching result is the fundamental goal.

The processed GNSS results are used as reference values. Only the velocity and position errors are presented and evaluated here, as the true attitude is difficult to obtain. The following definitions are made for simplicity.

Method 1: Pure INS solution.

Method 2: Comprehensive calibration of the INS using the matched position, considering that the vessel is relatively close to the coast at the initial stage, the gravity database has low accuracy, which affects matching performance; on the other hand, the INS itself has high accuracy and is trustworthy, so calibration can be omitted during this stage. Consequently, calibration is initiated after 24 h, and the strategy of calibration is to carry out the calibration as long as there is a matching position.

Method 3: Based on Method 2, only positions with high matching accuracy are selected for INS calibration. This is equivalent to adding judgment conditions to filter the matching positions.

Method 4: As described in Section 2.2, INS positioning error accumulates over time mainly due to the error in the longitude direction, and the longitude error is relatively independent of and not directly coupled to other state quantities. Therefore, this method focuses on longitude calibration. The latitude error mainly manifests as oscillation, although the oscillation amplitude gradually increases over time due to inertial sensor errors, its impact on INS positioning error is far smaller than that of longitude error. Moreover, the longer the INS operates, the more pronounced this phenomenon becomes. Consequently, in Method 4, only the longitude direction is calibrated; the latitude direction is not calibrated. This method is easy to implement in practice.

Figures 10 and 11 show the east and north velocity errors, respectively, while Figures 12–14 present the latitude, longitude, and position errors. The position error is a comprehensive consideration of both latitude and longitude errors. Since the INS comprehensive calibration starts at the 24th hour, the error curves for the first 24 h are identical. The results are summarized as follows.

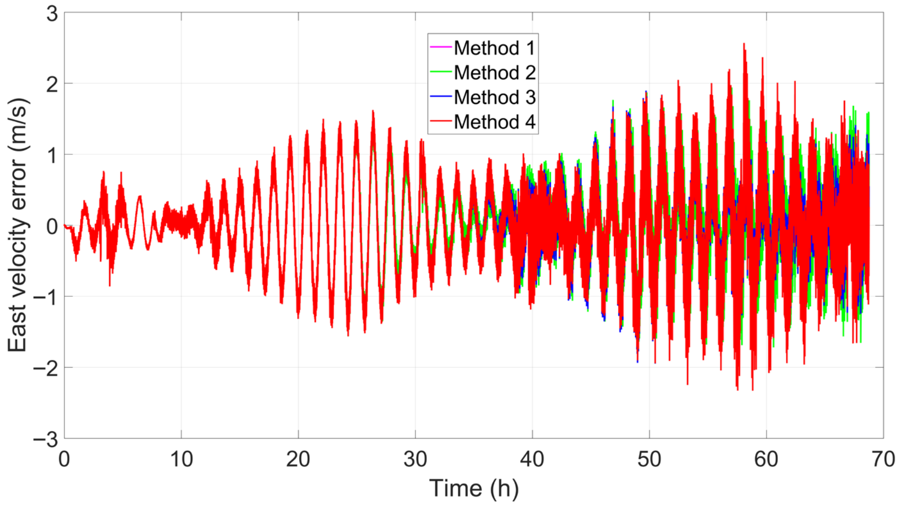

Figure 10. Comparison of east velocity errors for different methods in the shipboard test.

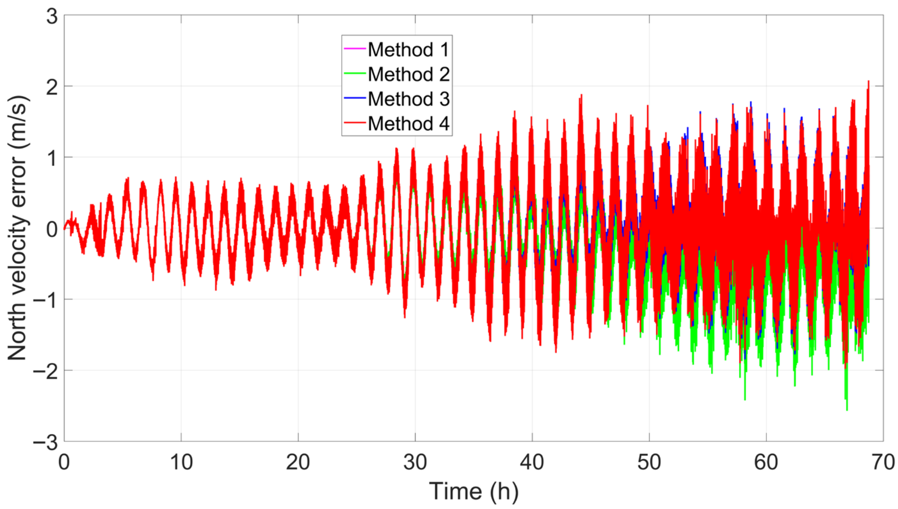

Figure 11. Comparison of north velocity errors for different methods in the shipboard test.

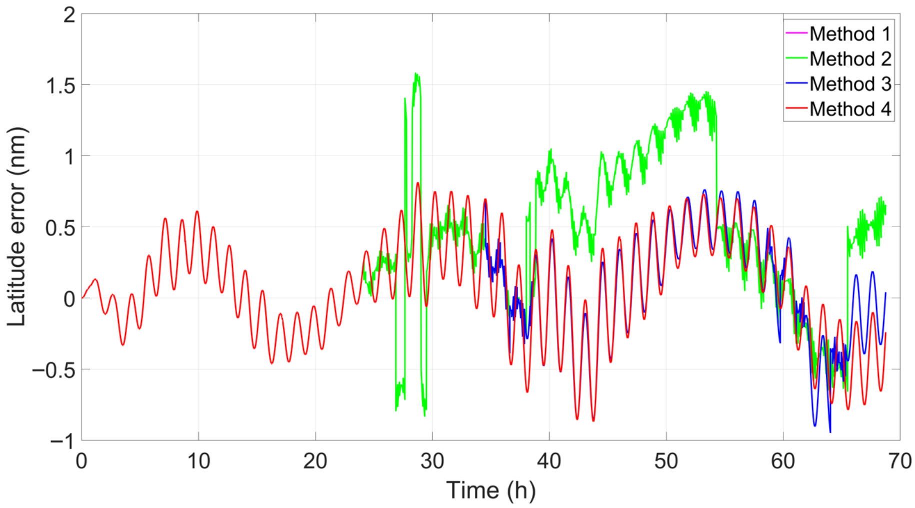

Figure 12. Comparison of latitude errors in different methods of shipboard test.

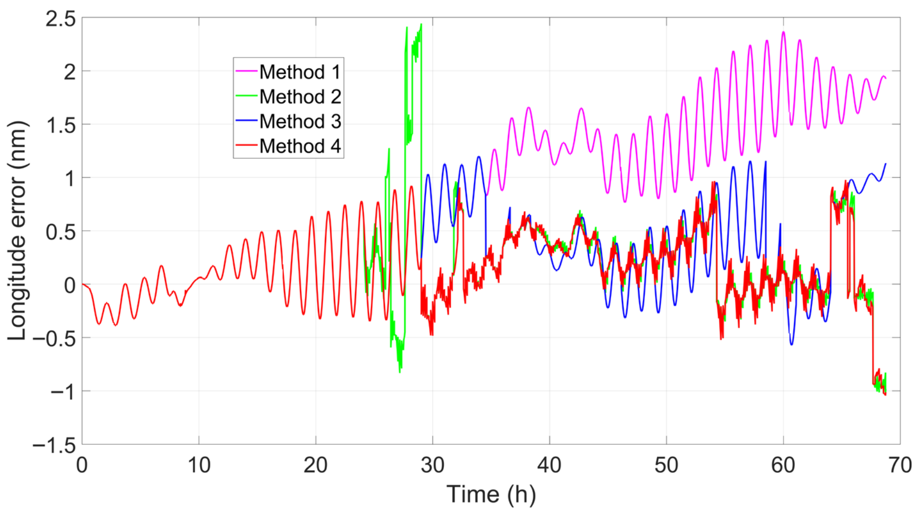

Figure 13. Comparison of longitude errors in different methods of shipboard test.

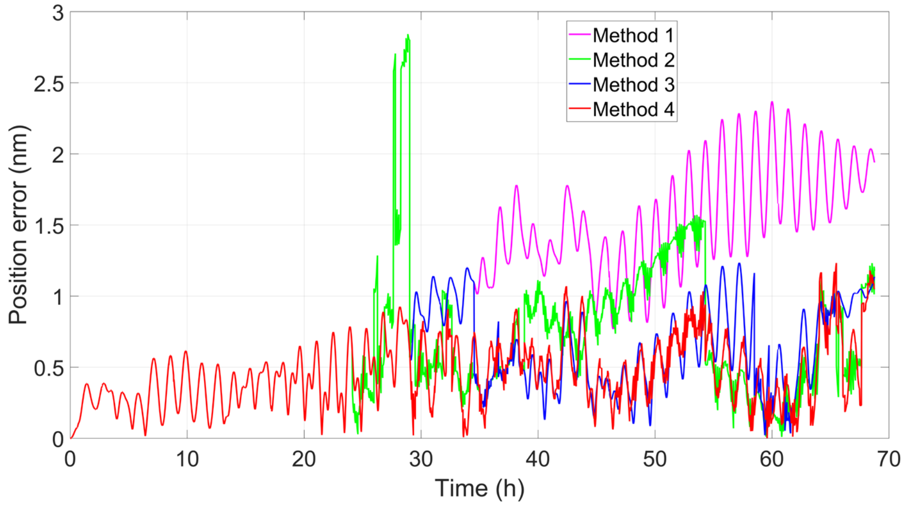

Figure 14. Comparison of position errors in different methods of shipboard test.

From the velocity error plots, it can be observed that: (1) there is still an obvious Schuler period oscillation error, because only the INS position is reset and no processing measures have been taken for the oscillating errors. This indicates that merely resetting the INS position does not suppress the Schuler period oscillation error; (2) the results of the four methods are presented together, making quantitative assessment from the figures difficult. Nevertheless, it is clear that different methods have different effects on velocity. This will be further analyzed later in conjunction with the statistical errors.

Regarding position error, the following observations can be made: (1) the position error exhibits Schuler period oscillation error, for the same reason as in the velocity error. (2) Method 2 imposes no constraints on the accuracy of the matched position; it essentially replaces the INS latitude and longitude directly with those obtained from matching. After comprehensive calibration, compared with Method 1, the accuracy improves in some areas but degrades in others. The result is unstable and prone to jumps. (3) Method 3 introduces constraints and selects only matched positions with high accuracy. Compared with Method 1, the latitude error is noticeable between approximately the 39th and 57th hours, and the longitude error between the 45th and 58th hours, as shown in Figures 12 and 13, during which the error trend is essentially the same as that of Method 1, indicating that no matching position satisfying the requirements is available. Compared with Method 2, although the error oscillates with a larger amplitude because adding constraints reduces the number of usable matched positions, the calibration effect is more consistent, and this consistency means that no abrupt jumps occur. (4) In Method 4, only the longitude direction is calibrated. There is no improvement in the latitude direction. However, the longitude accuracy is significantly improved compared with Method 1, and the effect is simultaneously more stable than that of Method 2 and more accurate than that of Method 3.

Figure 14 shows the position error of combined latitude and longitude, considering the consistency of error and oscillation amplitude of error, the effect of Method 4 is the best. Method 4 will be discussed in further detail later.

Next, the RMS values of velocity error and latitude error, as well as the maximum values of longitude error and position error, are calculated and presented in Tables 1 and 2, respectively.

Table 1. RMS error statistics of different methods.

Index	Method 1	Method 2	Method 3	Method 4
East velocity error (m/s)	0.6400	0.5634	0.6128	0.6400
North velocity error (m/s)	0.6020	0.6029	0.5818	0.6020
Latitude error (n mile)	0.4174	0.6953	0.4015	0.4174

Table 2. Maximum error statistics for different methods.

Methods	Longitude Error (n mile)	Position Error (n mile)
Method 1	2.3698	2.3699
Method 2	2.4427	2.8423
Method 3	1.1998	1.2352
Method 4	1.0449	1.2326

The RMS error statistics lead to conclusions essentially consistent with those previously drawn. Compared with Method 1, after applying Method 2, the RMS of the east velocity error decreases, whereas the RMS of the north velocity error and the latitude error increase. Method 3 reduces the RMS of the east velocity error, north velocity error, and latitude error compared with Method 1, and this improvement is consistent, because all selected matching positions have high accuracy. The statistics for Method 4 are identical to those for Method 1, indicating that open-loop calibration of only the longitude direction has no direct effect on these quantities.

For the error maximum statistics, compared with Method 1, Method 2 yields larger errors after processing, as shown in Figures 12–14, particularly between approximately the 26th and 30th hours. The maximum error of Method 3 is reduced, and Method 4 achieves higher accuracy than Method 3.

4. Discussion

In the above test, Method 4 achieved good results. Nevertheless, further analysis and verification are needed to determine whether it is the optimal method under various conditions. The following discussion summarizes the experience gained from this test and will serve as a reference for future tests.

1. This paper adopts open-loop calibration, which has the advantages of simplicity and ease of implementation.

The INS starts operating and reaches point A at time t_A, where a matching position P_A is obtained. After calibration, the INS error begins to accumulate from P_A. The INS then proceeds to point B at time t_B, where another matching position P_B is obtained. Following calibration, the INS error accumulates from P_B. If only the longitude component is chosen for calibration, theoretical analysis and data processing results indicate that this does not affect the solution of other INS parameters. If the error of P_A is relatively large, only the longitude error between t_A and t_B is affected. In this case, if the error of P_B is relatively small, the INS will be immediately pulled back to a comparatively correct position after calibration, ensuring that the impact of the matching position error remains limited.

If the latitude, velocities, and attitude angles are to be calibrated, they must be sufficiently accurate; otherwise, new errors will be introduced. These errors will affect other navigation parameters through the coupling relationship, and without correction, they will continue to accumulate and impact the INS in subsequent solution processes.

2. How to further improve accuracy is also one of the main research directions for future work.

In this paper, the focus has been on the suppression of longitude direction errors. Figures 10–12 show that the primary factors affecting east velocity, north velocity, and latitude accuracy are oscillatory errors, including Schuler oscillation modulated by the Foucault effect and Earth oscillation. In fact, damping network techniques are specifically used to suppress oscillatory errors [26,27]: horizontal damping networks suppress Schuler oscillation and simultaneously suppress the Foucault oscillation, while azimuth damping networks suppress Earth oscillation. Combining damping network techniques with the method proposed in this paper is expected to further improve navigation and positioning accuracy.

In addition, the test minimized dependence on GNSS signals. A platform-type gravimeter was used in the shipboard test, which required a dedicated control platform to provide a high-precision horizontal datum using combined INS/GNSS navigation during measurement, with an accuracy requirement better than 1 arcminute. GNSS signals were not used as an aid in the rest of the solution process; they served only as reference values for accuracy assessment. The calculation results suggest that in a real underwater environment, as long as gravity measurement accuracy reaches the same level or higher, good gravity matching performance can be achieved. This would enable comprehensive calibration of inertial navigation and improve its long-range navigation capability. Regarding the gravity instrument control platform, research indicates that technical solutions exist to provide a high-precision horizontal reference without relying on GNSS signals, which is crucial for underwater gravity measurement.

The surface test has provided valuable experience for the underwater test. In the future, a wider range of tests and validations will be conducted in different areas, both surface and underwater, without relying on GNSS signals at all, so as to advance gravity-assisted navigation toward engineering application.

5. Conclusions

This paper investigated an INS comprehensive calibration method using gravity-matched positions. The proposed approach adopts a direct position reset correction strategy designed for sparse and irregular measurement conditions in gravity-assisted navigation. The main conclusions are summarized as follows:

(1) The direct position reset strategy avoids the risk of Kalman filter divergence under sparse, low-accuracy measurement conditions. Each reset, when triggered, immediately eliminates the accumulated INS error.

(2) The shipboard test results show that after comprehensive calibration, the INS error can be maintained within 2 n mile. When Method 4 is adopted, which calibrates only the longitude direction, the maximum error does not exceed 1.5 n mile, and the error in most areas is better than 1 n mile. This represents a significant improvement over pure INS results and validates the effectiveness of the proposed method.

Future research will focus on several directions: (1) combining direct position reset with Kalman filtering fusion correction to achieve both fast convergence and smooth trajectory continuity; (2) introducing online sensor error estimation using least-squares-based parameter identification methods and Kalman filtering; and (3) extending the validation to more diverse geographic regions and longer mission durations to further assess the robustness and generalizability of the proposed method.

https://doi.org/10.3390/jmse14100925

Author Contributions: Conceptualization, Z.Z. and L.L.; methodology, Z.Z.; software, H.W. (Hubiao Wang); validation, X.L., G.W. and J.L.; formal analysis, Z.S.; investigation, J.W.; resources, L.L.; data curation, Z.S.; writing—original draft preparation, Z.Z.; writing—review and editing, J.W.; visualization, X.G.; supervision, H.W. (Huabing Wu); project administration, J.W.; funding acquisition, Z.Z. All authors have read and agreed to the published version of the manuscript.

Funding: This research was funded by the Open Foundation of the State Key Laboratory of Precision Geodesy, grant number SKLPG2025-4-2.

Data Availability Statement: The raw data supporting the conclusions of this article will be made. available by the authors on request.

Acknowledgments: We would like to express our sincere gratitude to the crew and staff of the R/V Dayang Hao for their invaluable assistance and support during the scientific expedition. We would also like to extend our sincere appreciation to the editor and the anonymous reviewers for their insightful comments and constructive suggestions, which have significantly contributed to the improvement and refinement of this work.

Conflicts of Interest: The authors declare no conflicts of interest.

Abbreviations

The following abbreviations are used in this manuscript:

INS	Inertial Navigation System
NTFT	Normal Time-Frequency Transform
GANT	Gravity-Assisted Navigation Technology
GNSS	Global Navigation Satellite System
GSS	Gravity Sensor System
GAINS	Gravity-Assisted Inertial Navigation System
NGS	Navigation and Gravity Systems
UGM	Universal Gravity Module
DVL	Doppler Velocity Log
DG	Depth Gauge

References

1. Bar-Itzhack, I.Y.; Berman, N. Control theoretic approach to inertial navigation systems. *J. Guid. Control Dyn.* **1988**, *11*, 237–245. [CrossRef] [PubMed]
2. Grewal, M.; Weill, L.; Andrews, A. *Global Positioning Systems, Inertial Navigation, and Integration*, 2nd ed.; Wiley-Interscience: Hoboken, NJ, USA, 2007.
3. Liu, P.; Wang, B.; Deng, Z.; Fu, M. INS/DVL/PS Tightly Coupled Underwater Navigation Method with Limited DVL Measurements. *IEEE Sens. J.* **2018**, *18*, 2994–3002. [CrossRef]
4. Li, K.; Zhu, T.; Chang, L.; Qian, L. Integrated positioning enhancement method based on nonlinear error model for the underwater multiply inertial navigation system. *Measurement* **2026**, *257*, 118944. [CrossRef]
5. Ben, Y.; Zang, X.; Li, Q.; Liu, X.; Chen, H. System reset for underwater strapdown inertial navigation system. *Ocean Eng.* **2019**, *182*, 552–562. [CrossRef]
6. Cai, S.; Tie, J.; Zhang, K.; Cao, J.; Wu, M. Marine gravimetry using the strapdown gravimeter SGA-WZ. *Mar. Geophys. Res.* **2017**, *38*, 325–340. [CrossRef]
7. Mao, N.; Li, A.; Xu, J.; Qin, F. A Multi-Resolution Sequence Method with Strong Constraints for Marine Gravity Matching Navigation. *J. Mar. Sci. Eng.* **2025**, *13*, 542. [CrossRef]
8. Koneshov, V.N.; Nepoklonov, V.B.; Avgustov, L.I. Estimating the navigation informativity of the Earth's anomalous gravity field. *Gyroscopy Navig.* **2016**, *7*, 277–284. [CrossRef]
9. Moryl, J.; Rice, H.; Shinners, S. The universal gravity module for enhanced submarine navigation. In *Proceedings of the IEEE 1998 Position Location and Navigation Symposium (Cat. No.98CH36153), 20–23 April 1996*; IEEE: New York, NY, USA, 1998; pp. 324–331.
10. Jircitano, A.; Dosch, D.E. Gravity aided inertial navigation system (GAINS). In *Proceedings of the 47th Annual Meeting of The Institute of Navigation (1991)*; Williamsburg Hilton and National Conference Center: Williamsburg, VA, USA, 1991; pp. 221–229.

11. Xiong, Z.; Cao, J.; Wu, M.; Cai, S.; Yu, R.; Wang, M. A Method for Underwater Dynamic Gravimetry Combining Inertial Navigation System, Doppler Velocity Log, and Depth Gauge. *IEEE Geosci. Remote Sens. Lett.* **2020**, *17*, 1294–1298. [CrossRef]
12. Han, Y.; Wang, B.; Deng, Z.; Wang, S.; Fu, M. A Mismatch Diagnostic Method for TERCOM-Based Underwater Gravity-Aided Navigation. *IEEE Sens. J.* **2017**, *17*, 2880–2888. [CrossRef]
13. Gannan, Y.; Hongwei, Z.; Kefei, Y.; Ling, Z. Improved SITAN algorithm in the application of aided inertial navigation. In *Proceedings of the 2012 International Conference on Measurement, Information and Control, Harbin, China, 18–20 May 2012*; IEEE: New York, NY, USA, 2012; pp. 922–926.
14. Han, Y.; Wang, B.; Deng, Z.; Fu, M. An Improved TERCOM-Based Algorithm for Gravity-Aided Navigation. *IEEE Sens. J.* **2016**, *16*, 2537–2544. [CrossRef]
15. Wang, Y.; Deng, Z.H.; Zhang, W.Z.; Zhao, S.W. An Improved ICCP Gravity Matching Algorithm Based on Mahalanobis Distance. In *Proceedings of the 2021 40th Chinese Control Conference (CCC), Shanghai, China, 26–28 July 2021*; IEEE: New York, NY, USA, 2021; pp. 3503–3508.
16. Wang, B.; Wu, L.; Wu, P.; Li, Q.; Bao, L.; Wang, Y. Multidimensional Evaluation of Altimetry Marine Gravity Models with Shipborne Gravity Data from a New Platform Marine Gravimeter. *J. Mar. Sci. Eng.* **2024**, *12*, 1314. [CrossRef]
17. Bishop, G.C. Gravitational field maps and navigational errors. In *Proceedings of the 2000 International Symposium on Underwater Technology (Cat. No. 00EX418), Tokyo, Japan, 26 May 2000*; IEEE: New York, NY, USA, 2000; pp. 149–154.
18. Rice, H.; Kelmenson, S.; Mendelsohn, L. Geophysical navigation technologies and applications. In *Proceedings of the PLANS 2004. Position Location and Navigation Symposium (IEEE Cat. No. 04CH37556), Monterey, CA, USA, 26–29 April 2004*; IEEE: New York, NY, USA, 2004; pp. 618–624.
19. Liu, H.; Wu, L.; Liu, S.; Xi, M.; Xiong, C.; Bao, L.; Wang, Y. A Flexible INS Correction on Method-Based Continuous and Sparse Gravity Matching Positions. *IEEE Trans. Instrum. Meas.* **2025**, *74*, 9512513. [CrossRef]
20. Sandwell, D.T.; Müller, R.D.; Smith, W.H.F.; Garcia, E.; Francis, R. New global marine gravity model from CryoSat-2 and Jason-1 reveals buried tectonic structure. *Science* **2014**, *346*, 65–67. [CrossRef] [PubMed]
21. Xi, B.; Yu, H.; Zhou, X. Compensation of ocean gravity measurement errors. *J. Chin. Inert. Technol. Eng.* **2011**, *19*, 1–5.
22. Zhou, Z.; Liang, X.; Shi, Z.; Wang, G.; Lang, J.; Liu, L. A New Method to Restrain Schuler Periodic Oscillation in Inertial Navigation System Based on Normal Time–Frequency Transform. *IEEE Trans. Instrum. Meas.* **2022**, *71*, 8502215. [CrossRef]
23. Sandwell, D.T.; Harper, H.; Tozer, B.; Smith, W.H.F. Gravity field recovery from geodetic altimeter missions. *Adv. Space Res.* **2021**, *68*, 1059–1072. [CrossRef]
24. Wang, H.; Wu, L.; Chai, H.; Bao, L.; Wang, Y. Location Accuracy of INS/Gravity-Integrated Navigation System on the Basis of Ocean Experiment and Simulation. *Sensors* **2017**, *17*, 2961. [CrossRef] [PubMed]
25. Zhu, C.; Guo, J.; Yuan, J.; Jin, X.; Gao, J.; Li, C. Refining Altimeter-Derived Gravity Anomaly Model from Shipborne Gravity by Multi-Layer Perceptron Neural Network: A Case in the South China Sea. *Remote Sens.* **2021**, *13*, 607. [CrossRef]
26. Cheng, J.H.; Zou, J.B.; Wu, L.; Hao, Y.L.; Gan, S.A. The design of an effective marine inertial navigation system scheme. In *Proceedings of the First International Workshop on Knowledge Discovery and Data Mining*; IEEE: New York, NY, USA, 2007; pp. 671–676.
27. Liu, C.; Wu, Q.P.; Hu, P.D.; Zhang, R. Design of Variable Damping INS for Ships Based on the Variation of Reference Velocity Error. *J. Sens.* **2021**, *2021*, 6628073. [CrossRef]